JOURNAL OF AGRICULTURAL AND FOOD CHEMISTRY

Double Phosphorylation of the Myosin Regulatory Light Chain during Rigor Mortis of Bovine Longissimus Muscle

SUSUMU MUROYA,*,† MAYUMI OHNISHI-KAMEYAMA,‡ MIKA OE,† IKUYO NAKAJIMA,§ MASAHIRO SHIBATA,|| AND KOICHI CHIKUNI†

Meat Protein Research Team and Animal Product Research Team, National Institute of Livestock and Grassland Science, Tsukuba, Ibaraki 305-0901, Mass Analysis Laboratory, National Food Research Institute, Tsukuba, Ibaraki 305-8642, and Meat Protein Research Team, National Agricultural Research Center for Western Region, Ohda, Shimane 694-0013, Japan

To investigate changes in myosin light chains (MyLCs) during postmortem aging of the bovine longissimus muscle, we performed two-dimensional gel electrophoresis followed by identification with matrix-assisted laser desorption ionization time-of-flight mass spectrometry. The results of fluorescent differential gel electrophoresis showed that two spots of the myosin regulatory light chain (MyLC2) at pI values of 4.6 and 4.7 shifted toward those at pI values of 4.5 and 4.6, respectively, by 24 h postmortem when rigor mortis was completed. Meanwhile, the MyLC1 and MyLC3 spots did not change during the 14 days postmortem. Phosphoprotein-specific staining of the gels demonstrated that the MyLC2 proteins at pI values of 4.5 and 4.6 were phosphorylated. Furthermore, possible N-terminal region peptides containing one and two phosphoserine residues were detected in each mass spectrum of the MyLC2 spots at pI values of 4.5 and 4.6, respectively. These results demonstrated that MyLC2 became doubly phosphorylated during rigor formation of the bovine longissimus, suggesting involvement of the MyLC2 phosphorylation in the progress of beef rigor mortis.

KEYWORDS: Bovine; myosin regulatory light chain (RLC, MyLC2); phosphorylation; rigor mortis; skeletal muscle

INTRODUCTION

Meat tenderness is one of the most important traits of meat quality (*1*). In postmortem skeletal muscles, continuous tension development accelerates the interdigitation of sarcomeric thin and thick filaments to an extreme extent, under the exhaustion of ATP and the release of Ca^{2+} from the sarcoplasmic reticulum. This muscle shortening determines the ultimate sarcomere length at rigor mortis, and the shortened sarcomere length has a great influence on meat tenderness (*2*, *3*). Numerous studies have shown that completion of rigor mortis at 10−18 °C was associated with minimum sarcomere shortening and maximum aging potential and resulted in the most tender meat (*3*−*7*). In the process of rigor mortis and the resolution, factors regulating or modulating muscle contraction could be involved in the sarcomere shortening and therefore could be able to change the meat tenderness.

In muscle contraction, myosin, a major protein of the myofibrillar thick filaments, plays a pivotal role in the force generation together with actin (*8*). The myosin molecule in the filaments consists of two heavy chains (MyHCs) and four light chains (MyLCs). Each of the N-termini of the MyHCs forms a globular domain, called the myosin head or subfragment 1 (S1), which contains a pair of the essential (ELC, or MyLC1) and the regulatory (RLC, or MyLC2) light chains.

While smooth muscle contraction is caused and regulated by MyLC2 phosphorylation with Ca^{2+}/calmodulin (CaM) activated myosin light chain kinase (MLCK) (*9*−*11*), the contraction in striated muscles is activated and regulated via sarcomeric thin filament proteins tropomyosin (Tm) and troponin (Tn), which includes a Ca^{2+}-sensitive subunit troponin C (*12*). Under the stimulation of Ca^{2+} release in sarcoplasm, the interaction between Tm and Tn modulates cyclic cross-bridge (actin−S1) interactions that, coupled with MgATP hydrolysis, result in sliding of the thin and thick filaments against each other and lead to force generation.

Unlike in smooth muscles, MyLC2 of striated muscles does not play a major regulatory role (*8*). However, the removal of MyLC2 from skeletal muscle fibers decreases the rate of force development, and the decrease was reversed by reincorporation of MyLC2 (*13*). In in vitro motility assays, removal of MyLC2 from skeletal muscle myosin also reduced the velocity of single actin filaments migrating on a myosin-coated surface (*14*). The velocity of actin movement was restored upon reconstitution

* To whom correspondence should be addressed. Phone: +81-(0)29-838-8686. Fax: +81-(0)29-838-8683. E-mail: muros@affrc.go.jp.
† Meat Protein Research Team, National Institute of Livestock and Grassland Science.
‡ National Food Research Institute.
§ Animal Product Research Team, National Institute of Livestock and Grassland Science.
|| National Agricultural Research Center for Western Region.

10.1021/jf063200o CCC: $37.00 © 2007 American Chemical Society
Published on Web 04/13/2007

of myosin with MyLC2. Thus, there are numerous observations that suggest a role for MyLC2 in the regulation of contraction.

Furthermore, such roles of MyLC2 have been clarified to be modulated by MyLC2 phosphorylation (*8*). In striated muscle, the MyLC2 phosphorylation is generally caused by MLCK (*15*) and correlates with potentiation of the maximal extent of the isometric twitch tension (*16*). It also increases the rate of force development (*17*−*19*) and the isometric tension (*20*) produced using reconstituted thin filaments or in skinned fibers at a submaximal Ca^{2+} concentration. Moreover, the force of fully Ca^{2+}-activated fast and slow skeletal muscle fibers can increase further by about 40% upon MyLC2 phosphorylation, and the MyLC2 phosphorylation partially reversed the inhibitory effect of 2,3-butanedionemonoxime on fiber tension (*21*).

Recently, postmortem changes in skeletal muscle MyLC2 on two-dimensional gel electrophoresis (2DE) have been reported (*22*, *23*). Despite the possibility of MyLC2 phosphorylation or dephosphorylation, no scientific evidence has been obtained concerning MyLC2 phosphorylation so far. To understand involvement of MyLC in sarcomere shortening during rigor mortis formation, the postmortem changes in bovine MyLC proteins were analyzed in this study. For analysis of the changes in protein modification, 2DE followed by spot identification with matrix-assisted laser desorption ionization time-of-flight mass spectrometry (MALDI-TOF MS) was performed.

MATERIALS AND METHODS

Animals and Muscle Samples. The animals were cared for as outlined in the *Guide for the Care and Use of Experimental Animals* (Animal Care Committee of the National Institute of Livestock and Grassland Science). Three Holstein cows aged 39−40 months were slaughtered after a brain concussion induced by captive-bolt gun stunning. For samples within 24 h postmortem, approximately 1 cm^3 pieces of M. longissimus thoracis (LT) were excised from the hanging carcasses and frozen in liquid nitrogen at 0 or 2 (treated as 0), 8, and 24 h after slaughter. After overnight hanging of the carcasses at 2 °C, an LT block was excised from each carcass and was bagged during aging at 2 °C. At 7 and 14 d postmortem, approximately 1 cm^3 pieces of the LT samples were prepared from the central part of the block.

Preparation of Myofibril Proteins. For myofibril preparation, each of the approximately 1 cm^3 muscle samples was minced and homogenized with homogenizing buffer, 20 mM potassium phosphate buffer (pH 6.8) containing 100 mM KCl, 1 mM $MgCl_2$, 1 mM EDTA, 1 mM 2-mercaptoethanol, and 0.05% sodium azide. In all steps of the myofibril preparation, the samples were kept on ice. The samples were washed twice in homogenizing buffer and once in 10 mM Tris−HCl (pH 8.0) containing 5 mM EDTA by centrifugation at 1000*g* for 15 min. Then the samples were solubilized in lysis buffer containing 8 M urea, 50 mM dithiothreitol (DTT), 4% CHAPS, and 0.2% Bio-Lyte 3/10 Ampholyte (Bio-Rad, California).

Two-Dimensional Electrophoresis (2DE). After the protein concentration was determined with a BCA protein assay reagent (Pierce, Illinois), the samples were loaded onto 11 cm long, pH 3−10 or 3−6 nonlinear and immobilized pH gradient (IPG) strips (Bio-Rad ReadyStrip). Isoelectric focusing (IEF) was performed in a Protean IEF cell (Bio-Rad). A certain amount of protein (50 and 200−500 μg) was used for phosphoprotein staining and MALDI-TOF MS, respectively. The strips were rehydrated overnight. For the subsequent IEF, voltage was increased gradually up to 8000 V for 2.5 h and then was maintained at a total voltage of 35000 or 50000 V.

Prior to the second dimensional SDS−PAGE, the strips were equilibrated for 20 min followed by 20 min in a solution of 6 M urea, 20% (v/v) glycerol, 2% SDS, and 50 mM Tris (pH 7.5), supplemented successively with 1% (w/v) DTT or 2.5% iodoacetamide. The SDS−PAGE was performed in a Criterion cell (Bio-Rad) on 12.5% polyacrylamide gel at 100 V for 1 h. Overall proteins in a preparative gel for MALDI-TOF mass analysis were stained in SYPRO Ruby (Bio-Rad). The experimental isoelectric point (pI) was determined using a 2DE protein standard (Bio-Rad).

Detection of Phosphorylated Spots. After 2DE, the proteins on the gel were fixed with 50% methanol and 10% acetic acid, and the gel was washed with water. According to the manufacturer's protocol, the gel was then stained with Pro-Q Diamond phosphoprotein gel stain (Invitrogen, Eugene, OR). After the gel was destained with 20% acetonitrile and 50 mM sodium acetate (pH 4.0) and washed with water, the fluorescence of the gel was scanned at an excitation of 540 nm and an emission of 595 nm with an Ettan DIGE Primo system (GE Healthcare, Fairfield, CT).

Fluorescent 2D Differential Gel Electrophoresis (DIGE). Myofibril samples at slaughter and aged 14 days postmortem were labeled with CyDye DIGE Fluor Cy3 and Cy5 minimal dyes (GE Healthcare), respectively, according to the manufacturer's protocol. Both samples (50 μg each) were mixed together and applied to 2DE as described above. After 2DE, the fluorescence of labeled proteins on the gel was scanned at Cy3 and Cy5 detection modes with the Ettan DIGE Primo system. After scanning of the SYPRO Ruby-stained gel image, the spot intensity was quantified with PDQuest software (Bio-Rad). The intensity was normalized with the total intensity of all protein spots on the gel.

MALDI-TOF MS. Protein spots of interest were manually excised from the SYPRO Ruby-stained gel in a clean air cabinet. The proteins in the gel pieces were subjected to reductive alkylation by iodoacetamide and digested with trypsin. The peptides were desalted using ZipTip C18 pipet tips (Millipore) and eluted with a matrix solution (α-cyano-4-hydroxycinnamic acid) onto the MALDI target. Mass spectra were recorded in the reflectron mode of a MALDI-TOF mass spectrometer (REFLEX II, Bruker Daltonics, Bremen, Germany) equipped with delayed extraction by summing 200 laser shots of a 337 nm nitrogen laser with an acceleration voltage of 20 kV. The mass spectrometer was calibrated externally once every eight samples using a commercially available peptide mixture (Bruker Daltonics) covering the 700−3200 *m*/*z* range. The obtained mass spectra were analyzed with XMASS 5.0 or FlexAnalysis 2.2 (Bruker Daltonics) software and transferred to a MASCOT peptide mass fingerprinting (PMF) search engine (Matrix Science, London, U.K.) through the BioTools program (Bruker Daltonics) to automatically search the NCBInr (National Center for Biotechnology Information nonredundant) database. The parameters were set to allow one or two miss cleavages with the enzyme trypsin and a peptide mass tolerance of 100−200 ppm.

Amino Acid Sequence Analysis of Possible Phosphorylated Peptides. Proteins in spots of interest excised from the SYPRO Ruby-stained gel were subjected to reductive alkylation by iodoacetamide and digested with trypsin. Possible phosphorylated peptides were detected in LC−nanoelectrospray ionization (nanoESI) MS/MS analysis (GeneWorld, Tokyo, Japan, http://www.geneworld.co.jp/). After the peptides were picked up, the amino acid sequences were further analyzed by MS/MS fragmentation (GeneWorld).

Statistical Analysis. The data were analyzed in a one-way factorial arrangement by ANOVA using JavaScript-STAR software (ver. 2.8.1, http://www.kisnet.or.jp/nappa/software/star/, 2000). When the effect was significant ($P < 0.05$), the means for each spot of interest were compared among days postmortem by the least significant difference method.

RESULTS

The pI of MyLC2 Shifted to Acidic Accompanying Beef Aging. First, we attempted to find changes in the myofibril proteins during postmortem aging of the bovine longissimus muscle. For this purpose, fluorescent 2D DIGE was conducted to compare at slaughter (0 d) with at 1 and 14 d beef myofibril composition. The results showed that MyLC2 at 0 d colored in green was at pI values of 4.65 and 4.76, while those at 1 and 14 d colored in red were at pI values of 4.53 and 4.65 (**Figure 1**). At a pI of 4.65, the spots of 0 and 1 d proteins or the spots of 0 and 14 d proteins overlapped at the same spot (7601), which made the spot colored yellow. This means that MW = 18800 spots were present at pI values of 4.65 (spot 7601) and 4.76

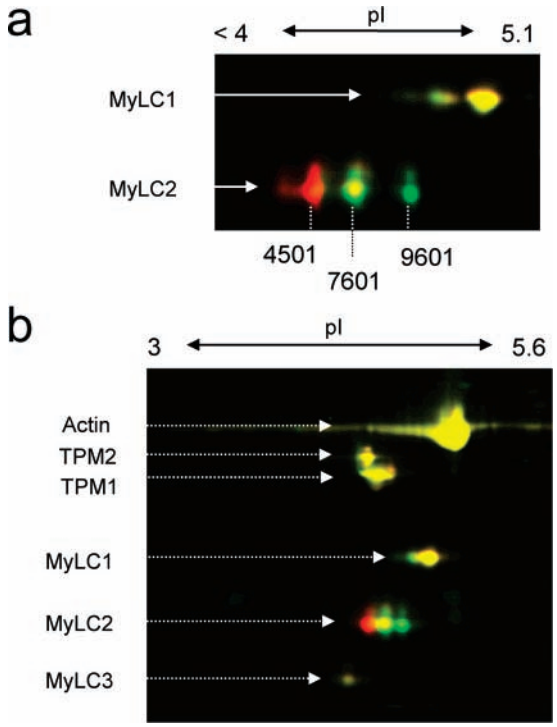

Figure 1. Changes in the two-dimensional electrophoretic gel image of bovine myofibril proteins during postmortem aging: (**a**) an area around MyLC2 spots (pI range 3–6), (**b**) whole gel image (pI range 3–10). The 0 and 14 d samples (**a**) or 0 and 1 d (24 h) samples (**b**) were labeled with Cy3 (green) and Cy5 (red), respectively, and applied to fluorescent differential gel electrophoresis. Overlapped spots of both samples are colored yellow. MyLC1, MyLC2, and MyLC3 = myosin light chains 1, 2, and 3. TPM1 and TPM2 = tropomyosins 1 and 2. Major MyLC2 spots are numbered as 4501, 7601, and 9601 for identification.

(spot 9601) at 0 d, whereas spot 9601 was faint and a spot at a pI of 4.53 (spot 4501) appeared at 1 or 14 d postmortem. Spots 4501, 7601, and 9601 were identified as MyLC2 with MALDI-TOF MS, showing the sequence coverage of 50.0−56.5% (**Table 1**). These spots were concluded to be fast-type isoforms (MyLC2f; *26*), according to the amino acid sequence homology of the matched bovine sequence (gi:76653375) to those of other species. The theoretical pI of bovine MyLC2f was estimated to be 4.73, but the experimental pI values of spots 4501 and 7601 were 4.53 and 4.65, respectively. These results indicated that the MyLC2 proteins underwent a pI shift from 4.76 to 4.53 during beef aging, possibly caused by phosphorylation. Minor spots with a higher molecular weight (19200) just above the MyLC2f spots were the slow-type isoforms (MyLC2s, unpublished data). The pI of MyLC2s also shifted toward the acidic region in the same manner as that of MyLC2f. Compared to this, spots of myosin light chains 1 (MyLC1) and 3 (MyLC3) were colored in yellow in the DIGE result, showing that they did not change at all during the beef aging (**Figure 1b**).

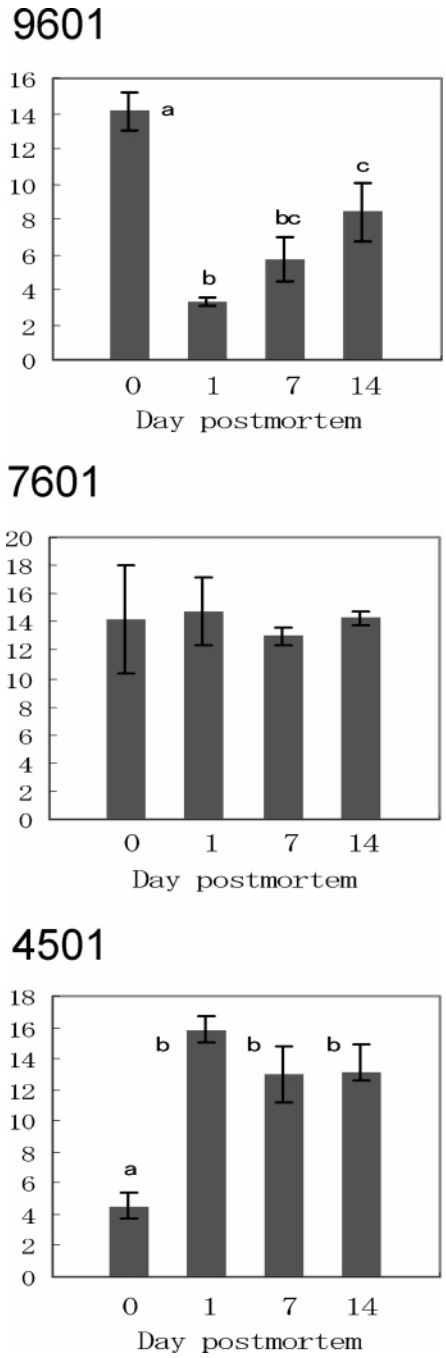

Figure 2. Changes in the spot intensity of MyLC2. The intensity of the gel spots was quantified with a densitometric method and statistically analyzed ($n = 3$). The unit of spot intensity (vertical axis) is arbitrary.

According to the quantitative analysis of the pI shift of MyLC2f, the intensity of spot 9601 at 0 d was significantly higher than that at 1, 7, and 14 d ($P < 0.05$), though the intensity gradually increased from 1 to 14 d to some extent (**Figure 2**).

Table 1. Summary of Mass Spectrometry Analysis of Myosin Light Chain 2-Related Spots

spot no.	appearance (day)	expl MW/pI	identification	sequence coverage (%)	theoretical MW/pI
4501	0	18800/4.53	MyLC2 (gi:76653375)	N.D.	19000/4.73
7601	0	18800/4.65	MyLC2 (gi:76653375)	56.5	19000/4.73
9601	0	18800/4.76	MyLC2 (gi:76653375)	56.5	19000/4.73
4501	14	18800/4.53	MyLC2 (gi:76653375)	50.0	19000/4.73
7601	14	18800/4.65	MyLC2 (gi:76653375)	56.5	19000/4.73
9601	14	18800/4.76	MyLC2 (gi:76653375)	56.5	19000/4.73

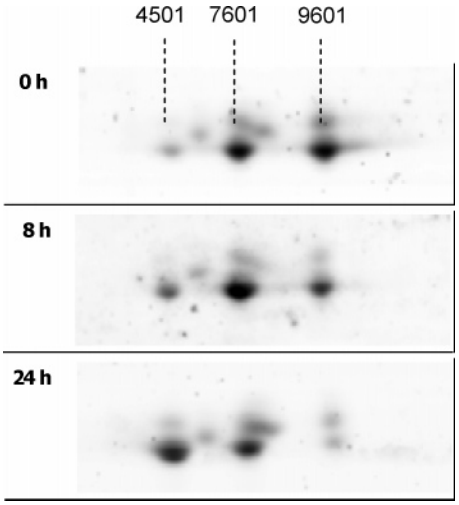

Figure 3. Changes in the pI of MyLC2 spots within 24 h postmortem. Major MyLC2 spots are numbered as 4501, 7601, and 9601 for identification. The sampling time is indicated on the left side.

In contrast to this, the intensity of spot 4501 at 0 d was significantly lower than that at 1, 7, and 14 d ($P < 0.05$), but no significant increase in the intensity was observed from 1 to 14 d. The intensity of spot 7601 did not change during postmortem aging.

In accordance with the result, the pI of the MyLC2f spot gradually shifted from 4.76 to 4.53 within 24 h after slaughter (**Figure 3**). At 0−2 h, most of the MyLC2f proteins were spotted at 9601 and 7601. At 8 h, a relatively high amount of MyLC2f was spotted at 7601, which indicates that the MyLC2f protein shifted to acidic via the intermediate form at a pI of 4.65. Thereafter, MyLC2f shifted further to a pI of 4.53 at 24 h. Thus, the pI of MyLC2f shifted to 4.53 by 1 d postmortem and did not seem to shift further thereafter. Therefore, it is likely that the pI of 4.53 was an ultimate form of MyLC2f during bovine muscle shortening.

Both Acidic and Intermediate pI Spots of MyLC2 Were of Phosphoproteins. The pI shift of MyLC2f was expected to be caused by protein phosphorylation. To examine this, the phosphoprotein spots on the 2DE gel were detected by phosphorylation-specific staining. The result of the staining showed that, throughout the entire aging process, only MyLC2f spots 4501 and 7601 were phosphorylated (colored yellow, **Figure 4**). Similarly, the MyLC2s spots at pI values of 4.53 and 4.65 were phosphorylated at all stages tested. However, MyLC2f spot 9601 and the MyLC2s spot at a pI of 4.76 were not found to be phosphorylated. Compared to MyLC2, MyLC1 and MyLC3 were not phosphorylated at all over the aging process.

This was consistent with the results of MALDI-TOF MS, where the mass of peptide modified with phosphorylation could successfully be detected. *m*/*z* 2481.2, 2560.8, and 2640.7 were detected from the tryptic digests of spots 9601, 7601, and 4501, respectively (**Figure 5**). Each of these peptides was specific to the respective spot, whereas most of the other peptides were shared in common among the spots. The difference in mass between spots 4501 and 7601, or spots 7601 and 9601, was approximately 80.0, just corresponding to the mass 79.98 which is added when an amino acid is phosphorylated. These results indicate that, first, the unphosphorylated form of MyLC2f at spot 9601 shifted to the monophosphorylated form at spot 7601 and then further shifted to the diphosphorylated form at spot 4501 by addition of a phosphate moiety one after another.

Actually, the phosphorylatable peptide AAAEGGSSSVFSMFDQTQIQEFK was observed at *m*/*z* 2481.2 (unphosphorylated form), where Met22 was supposed to be oxidized (**Figure 6**), and contains four serine residues. The peptide sequence was located at the N-terminal region of MyLC2f and contains Ser16 corresponding to Ser16 in rabbit MyLC2f (gi:127176) and Ser15 in mouse MyLC2f (gi:7949078), the primal phosphorylation site for modulation of skeletal muscle contraction (*8*, *27*, *28*).

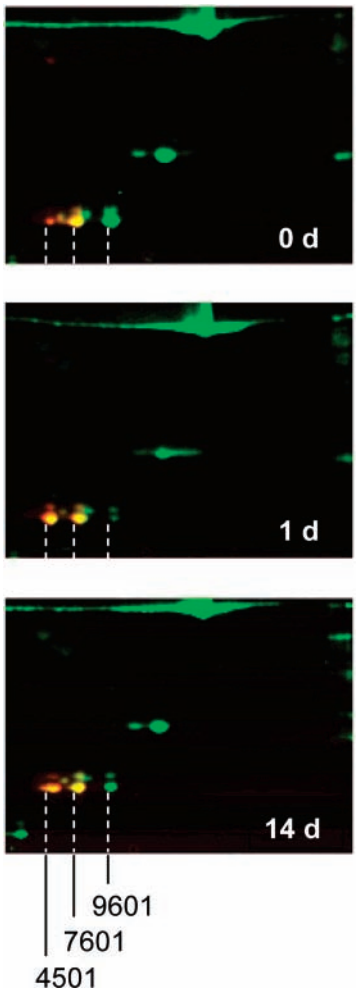

Figure 4. Distribution of myofibril phosphoproteins on a two-dimensional electrophoretic gel. Total proteins at 0, 1, and 14 d postmortem were stained with SYPRO Ruby (green), and phosphoproteins were doubly stained with SYPRO Ruby and Pro-Q Diamond (yellow). Weak spots above MyLC2f spots 4501, 7601, and 9601 are of MyLC2s.

This peptide is estimated to have *m*/*z* 2561.0 with a single phosphorylation and to have *m*/*z* 2640.8 with double phosphorylation. The *m*/*z* values of the peptides detected from spots 7601 and 4501 were in agreement with the theoretical values of the phosphorylated peptides. According to collision-induced fragmentation spectra (MS/MS) of the possible phosphopeptides, signals corresponding to the carboxy-terminal eight and ten amino acid residues were detected from peptides *m*/*z* 2561.0 and 2640.8, respectively (data not shown). Although none of the phosphorylated sites were determined, the result indicated that both *m*/*z* 2561.0 and 2640.8 peptides were modified forms of the peptide AAAEGGSSSVFSMFDQTQIQEFK.

Furthermore, to examine the extent of phosphorylation of the spots, we calculated the intensity ratio of Pro-Q Diamond staining/SYPRO Ruby staining for spots 4501 and 7601 at 24 h postmortem. As a result of this, the ratio of the phosphorylation/protein content of spot 4501 was 1.84 times as high as that of spot 7601 ($P < 0.005$). This finding supports the result

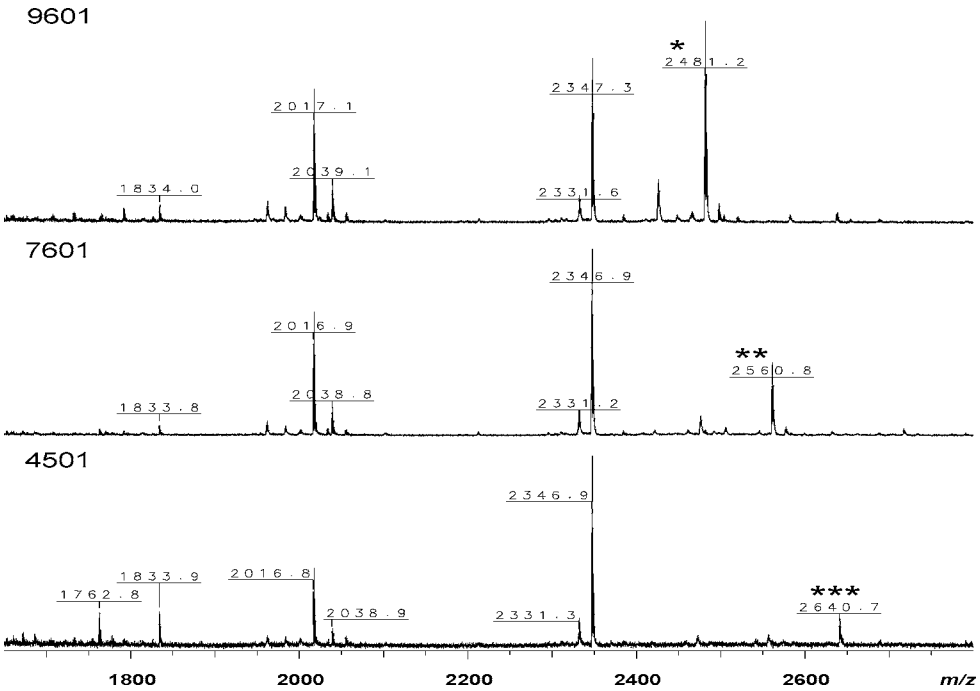

Figure 5. Mass spectra of MyLC2 spots analyzed on the MALDI-TOF mass spectrometer. Each peptide mass peak specific to the respective spot is marked with asterisks.

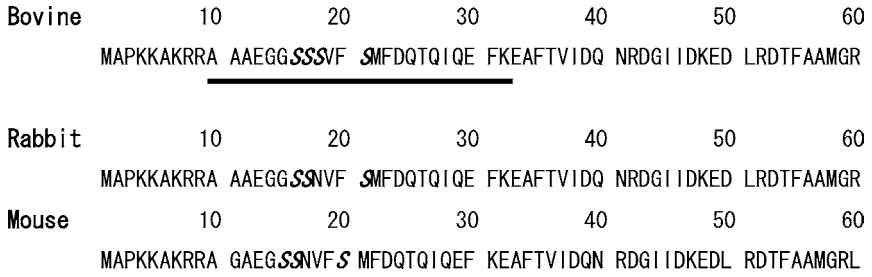

Figure 6. Potential phosphorylation sites on bovine MyLC2. The possible phosphorylated peptide region is underlined with a bold line. Serine residues for potential phosphorylation are bold and italic. NCBI database accession numbers: BG224056 for bovine, P02608 for rabbit, and NP_058034 or AAH55869 for mouse sequences.

that MyLC2 of spots 4501 and 7601 was of double and of single phosphorylation, respectively.

DISCUSSION

In this study, we have shown that MyLC2 phosphorylation occurred during postmortem rigor mortis of the bovine LT muscle. At slaughter, two types of MyLC2 proteins were present, one an unphosphorylated form of pI 4.76 and the other a singly phosphorylated form of pI 4.65. By 24 h postmortem, most of the MyLC2 proteins were phosphorylated at one or two sites and appeared as spots of pI 4.65 or 4.53 on 2DE gel. After 24 h postmortem, no significant change in MyLC2 phosphorylation was observed. The present data indicated that double MyLC2 phosphorylation occurred on the N-terminal region.

The spot pattern of the bovine MyLC2 forms observed here was in agreement with the previous result of the 2DE analysis (*24*, *25*). Lametsch et al. (*22*) and Morzel et al. (*23*) analyzed the effect of postmortem aging on pork proteome and also observed postmortem changes in MyLC2; however, it has never been demonstrated that MyLC2 is phosphorylated in postmortem skeletal muscle. Morzel et al. (*23*) hypothesized that MyLC2 was dephosphorylated because they observed the pI shift of the MyLC2 spot toward alkaline, while Lametsch et al. (*22*) did not reach any conclusion about the cause of the change in MyLC2. The spot that Morzel et al. (*23*) found to increase was the most alkaline, unphosphorylated form. As shown in the present results, unphosphorylated MyLC2 (spot 9601) gradually increased after 24 h postmortem (**Figure 2**), which does not contradict the result of Morzel et al. (*23*). This might reflect the gradual dephosphorylation of MyLC2 in beef after 24 h postmortem. However, in their study, the MyLC2 unphosphorylated form also increased from slaughter to 12 h postmortem. The reason for the difference in the MyLC2 change is unclear. The difference might be due to the difference in species between beef and pork. Generally, in porcine muscle, rigor mortis and postmortem aging progress at a rate less than half that of beef. It was possible that the MyLC2 phosphorylation was already over at 12 h postmortem in pork. Otherwise, the difference might be due to the use of myofibrils (present) or whole muscle proteins (previous). When whole muscle samples that include numerous sarcoplasmic proteins were used, some proteins' spots might have overlapped on the 2DE gel with the spot of MyLC2 in common, which could change the apparent amount of the spot.

There are numerous observations that suggest a role for the MyLC2 phosphorylation in the regulation of force development (*16*−*21*). Sweeney et al. (*15*) postulated that MyLC2 phosphorylation acts in vertebrate skeletal muscle as a factor enhancing the performance of muscle, a kind of "memory" that the muscle has recently been active. The MyLC2 phosphorylation enhances

the force if the muscle was previously activated and allows the force to be maintained at a certain level even if, during prolonged contractions, the Ca^{2+} concentration becomes decreased. Thus, the MyLC2 phosphorylation plays an important modulatory role in skeletal muscle contraction.

In skeletal muscle, the MyLC2 phosphorylation occurs at the N-terminal end, on serine 16 in rabbit MyLC2f (*8*, *27*) and serine 15 in mouse MyLC2f (*28*). Our present data indicated that MyLC2 phosphorylation occurs in postmortem skeletal muscle in a manner similar to that in live muscle. Whether a second site of phosphorylation is also present in sarcomeric MyLC2 was controversial (*29*, *30*). However, in this study, the presence of doubly phosphorylated MyLC2 was confirmed on the bovine skeletal muscle at 24 h postmortem. This is supported by the reports that showed the presence of doubly phosphorylated MyLC2 on 2DE gel in cases of the myostatin-deficient bovine muscles possessing a faster type property (*24*) and the slow-to-fast muscle phenotype type transition induced by clenbuterol treatment of rat soleus muscle (*25*). Furthermore, Hidalgo et al. (*31*) demonstrated that MyLC2 of tarantula striated muscle is phosphorylated at one or two sites, depending on the conditions of contraction.

We observed the coexistence of both un- and monophosphorylated MyLC2 at slaughter muscles that were still alive. This is consistent with the previous result showing that basal phosphorylation substantially occurs at the first site in relaxed muscles (*31*). Generally, after slaughter, rigor mortis of the bovine longissimus muscle is completed during 12−24 h postmortem at 1−7 °C (*32*). During the rigor mortis, actomyosin formation proceeds slowly at first (the delay phase) and then with great rapidity (the fast phase) in the rigor formation (*33*). In our results, the ratio of the phosphorylated form to unphosphorylated form increased by 24 h postmortem, possibly in parallel with the rigor formation. In particular, the appearance of the doubly phosphorylated form after 8 h postmortem seemed to coincide with the fast phase of rigor mortis. It has been reported that, on activation of muscle contraction, the basal phosphorylation increases first, which is followed by partial phosphorylation of the second site (*31*). Although the sites and role of double phosphorylation on MyLC2 are not clear, it is likely that the second phosphorylation plays an important role in strong sustainable muscle shortening.

The two-step phosphorylation was likely to be caused by the postmortem increase in the sarcoplasmic Ca^{2+} concentration, which is due to the release from no longer maintainable sarcoplasmic reticulum (*1*). Actually, Ca^{2+} influences MyLC2 phosphorylation in striated muscles in a concentration-dependent manner; at a low concentration (relaxing conditions) only basal phosphorylation occurs, while at higher concentrations (activating conditions) the MyLC2 phosphorylation is stimulated, although at a still higher concentration, partial inhibition of the phosphorylation is observed (*31*). The stimulation of MyLC2 phosphorylation with Ca^{2+} is mediated by Ca^{2+}/calmodulin-dependent MLCK (*15*). This mechanism of phosphorylation can well explain the present observation of phosphorylation in the postmortem bovine muscle, although the level of Ca^{2+} concentration in the bovine muscle was not determined during the rigor formation. Since the activities of MLCK and phosphatases could affect the MyLC2 phosphorylation, the effects of the activities and Ca^{2+} concentration require further analysis for the better understanding of the mechanism of phosphorylation in postmortem muscles.

The present DIGE results showed that MyLC1 and MyLC3 did not seem to change on the 2DE gel during 14 d of postmortem muscle aging, although a quantitative analysis was not performed. On the other hand, the degradation of pork MyLC1 (*22*, *34*) and the pI shift of pork MyLC3 (*23*) were observed at 3 or 7 d postmortem. In the conventional SDS−PAGE analysis of the postmortem degradation of myofibril proteins, there has been no other study that reported the degradation of MyLC. The difference in MyLC1 between the present and previous results might be due to the presence of sarcoplasmic proteins in the samples, as described above. Likewise, MyLC3 might apparently change in the case using whole muscle proteins. Unlike MyLC2, there has never been a report on the functional phosphorylation of MyLC3 or on that of MyLC1. Actually, no phosphorylation was observed in the MyLC1 and MyLC3 spots during the beef aging in this study. In addition, in the DIGE system in which two different samples (at slaughter and at 14 d postmortem) labeled with different dyes were mixed and applied to one 2DE gel, there could be no wrong matching of spots due to the difference in gel distortion between the two separate gels. Therefore, analysis using DIGE has the advantage of being able to monitor changes in a specific spot accurately. Taken together, it is concluded here that MyLC1 and MyLC3 did not undergo postmortem modification or degradation.

ACKNOWLEDGMENT

We thank Tomoko Sato of the National Food Research Institute for technical help with the MS measurements.

LITERATURE CITED

(1) Lawrie, R. A. The eating quality of meat. In *Lawrie's Meat Science*, 6th ed.; Lawrie, R. A., Ed.; Woodhead Publishing Ltd.: Abington, Cambridge, England, 1998; Chapter 10, pp 212−257.

(2) Koohmaraie, M.; Doumit, M. E.; Wheeler, T. L. Meat toughening does not occur when rigor shortening is prevented. *J. Anim. Sci.* **1996**, *74*, 2935−2942.

(3) Tornberg, E. Biophysical aspects of meat tenderness. *Meat Sci.* **1996**, *43*, S175−S191.

(4) Devine, C. E.; Payne, S. R.; Peachey, B. M.; Lowe, T. E.; Ingram, J. R.; Cook, C. J. High and low *rigor* temperature effect on sheep meat tenderness and ageing. *Meat Sci.* **2002**, *60*, 141−146.

(5) Devine, C. E.; Wahlgren, N. M.; Tornberg, E. Effect of rigor temperature on muscle shortening and tenderization of restrained and unrestrained beef *m. longissimus thoracis* and *lumborum*. *Meat Sci.* **1999**, *51*, 61−72.

(6) Hwang, I. H.; Devine, C. E.; Hopkins, D. L. The biochemical and physical effects of electrical stimulation on beef and sheep meat tenderness. *Meat Sci.* **2003**, *65*, 677−691.

(7) Nuss, J. I.; Wolfe, F. H. Effect of post-mortem storage temperatures on isometric tension pH, ATP, glycogen and glucose-6-phosphate for selected bovine muscles. *Meat Sci.* **1980**, *5*, 201−213.

(8) Szczesna, D. Regulatory light chains of striated muscle myosin. Structure, function and Malfunction. *Curr. Drug Targets: Cardiovasc. Haematol. Disord.* **2003**, *3*, 187−197.

(9) Hartshorne, D. J.; Mrwa, U. Regulation of smooth muscle actomyosin. *Blood Vessels* **1982**, *19*, 1−18.

(10) Small, J. V.; Sobieszek, A. Ca-regulation of mammalian smooth muscle actomyosin via a kinase-phosphatase-dependent phosphorylation and dephosphorylation of the 20,000-Mr light chain of myosin. *Eur. J. Biochem.* **1977**, *76*, 521−530.

(11) Sobieszek, A. Ca-linked phosphorylation of a light chain of vertebrate smooth-muscle myosin. *Eur. J. Biochem.* **1977**, *73*, 477−483.

(12) Gordon, A. M.; Homsher, E.; Regnier, M. Regulation of contraction in striated muscle. *Physiol. Rev.* **2000**, *80*, 853−924.
(13) Szczesna, D.; Zhao, J.; Potter, J. D. The regulatory light chains of myosin modulate cross-bridge cycling in skeletal muscle. *J. Biol. Chem.* **1996**, *271*, 5246−5250.
(14) Lowey, S.; Waller, G. S.; Trybus, K. M. Skeletal muscle myosin light chains are essential for physiological speeds of shortening. *Nature* **1993**, *365*, 454−456.
(15) Sweeney, H. L.; Bowman, B. F.; Stull, J. T. Myosin light chain phosphorylation in vertebrate striated muscle: regulation and function. *Am. J. Physiol*. **1993**, *264*, C1085−1095.
(16) Houston, M. E.; Green, H. J.; Stull, J. T. Myosin light chain phosphorylation and isometric twitch potentiation in intact human muscle. *Pflügers Arch.* **1985**, *403*, 348−352.
(17) Metzger, J. M.; Greaser, M. L.; Moss, R. L. Variations in cross-bridge attachment rate and tension with phosphorylation of myosin in mammalian skinned skeletal muscle fibers. Implications for twitch potentiation in intact muscle. *J. Gen. Physiol.* **1989**, *93*, 855−83.
(18) Sweeney, H. L.; Stull, J. T. Phosphorylation of myosin in permeabilized mammalian cardiac and skeletal muscle cells. *Am. J. Physiol.* **1986**, *250*, C657−660.
(19) Szczesna, D.; Zhao, J.; Jones, M.; Zhi, G.; Stull, J.; Potter, J. D. Phosphorylation of the regulatory light chains of myosin affects Ca2+ sensitivity of skeletal muscle contraction. *J. Appl. Physiol.* **2002**, *92*, 1661−1670.
(20) Persechini, A.; Stull, J. T.; Cooke, R. The effect of myosin phosphorylation on the contractile properties of skinned rabbit skeletal muscle fibers. *J. Biol. Chem.* **1985**, *260*, 7951−7954.
(21) Davis, J. S.; Satorius, C. L.; Epstein, N. D. Kinetic effects of myosin regulatory chain phosphorylation on skeletal muscle contraction. *Biophys. J.* **2002**, *83*, 359−370.
(22) Lametsch, R.; Karlsson, A.; Rosenvold, K.; Andersen, H. J.; Roepstorff, P.; & Bendixen, E. Postmortem proteome changes of porcine muscle related to tenderness. *J. Agric. Food Chem.* **2003**, *51*, 6992−6997.
(23) Morzel, M.; Chambon, C.; Hamelin, M.; Santé-Lhoutellier, V.; Sayd, T.; Monin, G. Proteome changes during pork meat ageing following use of two different pre-slaughter handling procedures. *Meat Sci.* **2004**, *67*, 689−696.
(24) Bouley, J.; Meunier, B.; Chambon, C.; De Smet, S.; Hocquette, J. F.; Picard, B. Proteomic analysis of bovine skeletal muscle hypertrophy. *Proteomics* **2005**, *5*, 490−500.
(25) Bozzo, C.; Stevens, L.; Toniolo, L.; Mounier, Y.; Reggiani, C. Increased phosphorylation of myosin light chain associated with slow-to-fast transition in rat soleus. *Am. J. Physiol. Cell Physiol.* **2003**, *285*, 575−583.
(26) Schiaffino, S.; Reggiani, C. Myosin isoforms in mammalian skeletal muscle. *J. Appl. Physiol.* **1994**, *77*, 493−501.
(27) Herring, B. P.; Gallagher, P. J.; Stull, J. T. Substrate specificity of myosin light chain kinases. *J. Biol. Chem.* **1992**, *267*, 25945−25950.
(28) Zhi, G.; Ryder, J. W.; Huang, J.; Ding, P.; Chen, Y.; Zhao, Y.; Kamm, K. E.; Stull, J. T. Myosin light chain kinase and myosin phosphorylation effect frequency-dependent potentiation of skeletal muscle contraction. *Proc. Natl. Acad. Sci. U.S.A.* **2005**, *102*, 17519−17524.
(29) Gonzalez, B.; Negredo, P.; Hernando, R.; Manso, R. Protein variants of skeletal muscle regulatory myosin light chain isoforms: prevalence in mammals, generation and transition during muscle remodeling. *Pflügers Arch.* **2002**, *443*, 377−386.
(30) Morano, I.; Wankerl, M.; Bohm, M.; Erdmann, E.; Ruegg, J. C. Myosin-P-light chain isoenzymes in the human heart: evidence for a diphosphorylation of the atrial P-LC form. *Basic Res. Cardiol.* **1989**, *84*, 298−305.
(31) Hidalgo, C.; Craig, R.; Ikebe, M.; Padron, R. Mechanism of phosphorylation of the regulatory light chain of myosin from tarantula striated muscle. *J. Muscle Res. Cell Motil.* **2001**, *22*, 51−59.
(32) Olsson, U.; Hertzman, C.; Tornberg, E. The influence of low temperature, type of muscle and electrical stimulation on the course of rigor mortis, ageing and tenderness of beef muscles. *Meat Sci.* **1994**, *37*, 115−131.
(33) Lawrie, R. A. Chemical and biochemical constitution of muscle. In *Lawrie's Meat Science*, 6th ed.; Lawrie, R. A., Ed.; Woodhead Publishing Ltd.: Abington, Cambridge, England, 1998; Chapter 4, pp 58−95.
(34) Hwang, I. H.; Park, B. Y.; Kim, J. H.; Cho, S. H.; Lee, J. M. Assessment of postmortem proteolysis by gel-based proteome analysis and its relationship to meat quality traits in pig longissimus. *Meat Sci.* **2005**, *69*, 79−91.

Received for review November 7, 2006. Revised manuscript received February 15, 2007. Accepted March 7, 2007.

JF063200O